SEISMIC ANALYSIS OF REACTOR CONTAINMENT FACILITY FOR PWR PLANT (COUPLED VIBRATION WITH ATTACHED BUILDINGS)

T. TAKEMORI, I. HAMA

Taisei Corporation, Osaka Branch Office, Higashiku Osaka, Japan

SUMMARY

In seismic design of the reactor containment facility (hereinafter RCF) for a PWR nuclear power station, many structural problems occur; one of the problems is how to idealize the structure of this facility to a computable model, and another is whether to obtain the suitable computer program for seismic analysis.

In this paper a layout of a PWR nuclear power station is assumed referring to actual PWR power stations and the dynamic analyses are carried out making several dynamic models from it.

RCF has three independent structural components—Interior concrete structure, Steel containment vessel and Annulus shield wall. They are directly standing on the rigid foundation based on hard rock. Around this foundation, there are several attached buildings such as Auxiliary building and Intermediate building whose floor levels are different respectively. Some of them are partly connected with the foundation of RCF.

The structural models made from the layout are as follows.

Case 1: Interior concrete structure, Steel containment vessel and Annulus shield wall are idealized as a 2-lumped mass, 5-lumped mass and 5-lumped mass dynamic model, respectively, fixed on the top of foundation.

Case 2: Three components mentioned above and the foundation are idealized as a 14-lumped mass coupled dynamic model fixed on rigid bed rock.

Case 3: The model is identical to the model in case 2. However, rocking and swaying springs assumed in the bed rock are considered to the bottom of the foundation.

In the analyses of cases 1-3, computer programs of plane flexure—shear type are adopted.

Case 4: The model of case 3 is replaced by a space model and is combined with other space models representing the several attached buildings. The model is a 84 degree spaced system with 28-lumped mass.

As for case 4, the spaced dynamic analysis computer program developed by us is used in order to compare with cases 1-3.

Earthquake waves employed in this study are El Centro NS 40, Taft 52EW and Golden Gate S80E. The maximum accelerations of these waves are normalized to 250 gal.

Based on these results the variation of dynamic responses due to the difference of models are investigated to evaluate the dynamic analysis procedures.

1. Introduction

In this paper, a layout of PWR nuclear power station as shown in Fig.1 is assumed referring to existing PWR power stations, and analyses of time history responses due to the well known three earthquake waves are carried out making four dynamic structural models based on the layout as mentioned in chapter 2. The results of analyses on different four models excited by three earthquake waves are compared one another, and the effects of the horizontal interaction in the junction between the Reactor Containment Facility (hereinafter RCF) and the Attached Buildings (hereinafter AB), are discussed.

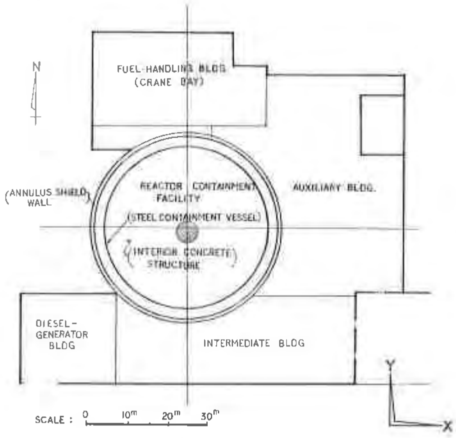

Fig.1 A layout of PWR nuclear power station

2. Dynamic Models

RCF consists of three independent structural components - Interior Concrete Structure (ICS), Steel Containment Vessel (SCV), and Annulus concrete Shield Wall (ASW). They are standing directly on the common rigid foundation based on the hard rock. Around this foundation, there are several attached buildings such as Auxiliary-building, Intermediate-building, and other buildings whose floor levels are different one another. Some of them are partly connected with the foundation of RCF.

The structural models made from the layout are as follows:

Case 1: (C - 1) ICS, SCV, and ASW are idealized as 2-lumped mass, 5-lumped mass, and 5-lumped mass dynamic models, respectively fixed on the top of the foundation. See Fig.2.

Case 2: (C - 2) Three components mentioned above with the foundation are idealized as a 15-lumped mass coupled dynamic model fixed on the hard rock. See Fig.3.

Case 3: (C - 3) Rocking and swaying springs are assumed situated in the hard rock underneath the foundation of model identical to Case 2. See Fig.4.

Case 4: (C - 4) The model of Case 3 is replaced by the space model and is combined with other space models representing the several attached buildings. The model is 87-degree-of-freedom space system with 29-lumped masses. See Fig.5.

3. Characteristics of Computer Program

In the analyses of Cases 1~3, computer programs for two-dimensional flexure-shear structure are adopted. The computer program used for Case 4 is developed for a dynamic analysis of three dimensional structure idealized as lumped mass system in which mode superposition method are used [1], [3].

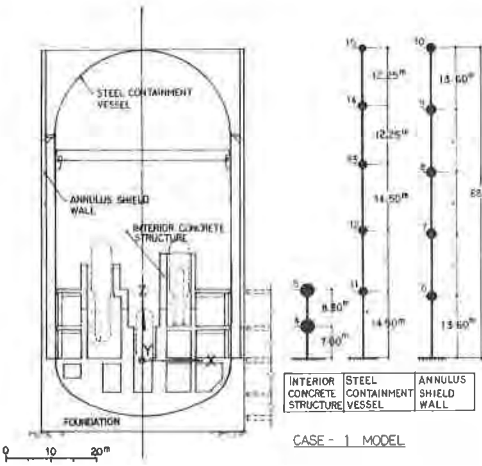

Fig.2 Case 1 - Structural model

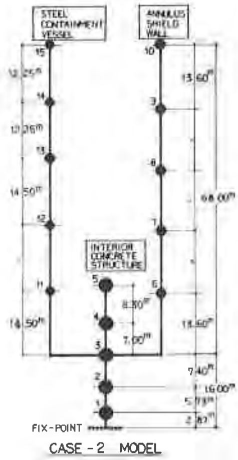

Fig.3 Case 2 - Structural model

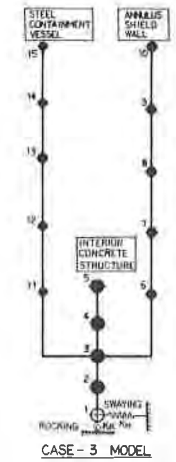

Fig.4 Case 3 - Structural model

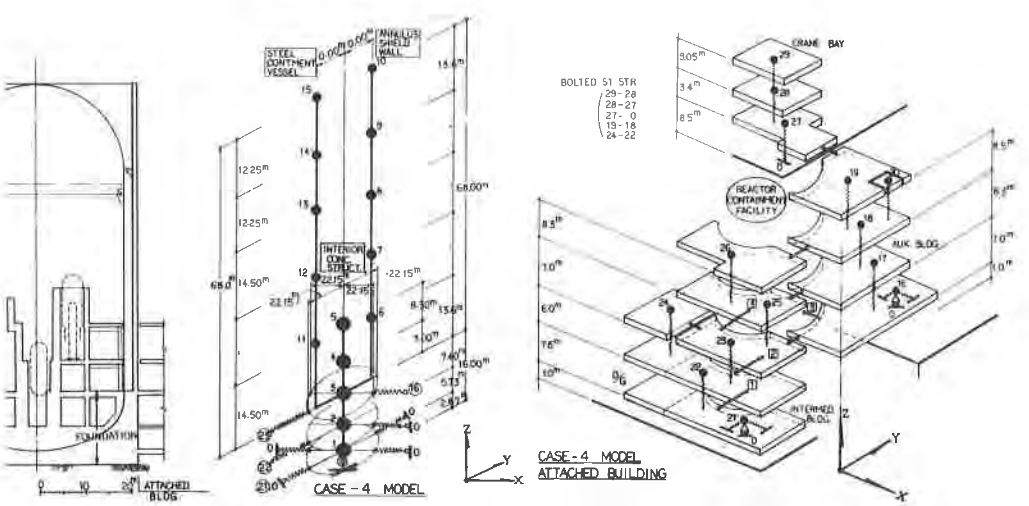

Fig.5 Case 4 - Structural model

The assumptions adopted are as follows:

(1) Floor slabs are assumed infinitely rigid.

(2) Vertical displacements are not considered.

(3) Structures are idealized as the lumped mass system.

(4) Mass moments of inertia about X and Y axes are neglected.

(5) Vertical resisting components in the horizontal springs (mainly floor slabs) between each mass are neglected.

4. Properties

Spring constants, masses, etc. are shown in Table I.

a) Materials:

Concrete;		Steel;	
Young's modulus	: $E_c = 2.1 \times 10^6 t/m^2$	Young's modulus	: $E_s = 2.1 \times 10^7 t/m^2$
Shear modulus	: $G_c = 0.89 \times 10^6 t/m^2$	Shear modulus	: $G_s = 0.81 \times 10^7 t/m^2$
Poisson's ratio	: $\nu_c = 0.1667$	Poisson's ratio	: $\nu_s = 0.3$
Specific gravity	: $\rho_c = 2.4 t/m^3$	Specific gravity	: $\rho_s = 7.85 t/m^3$

b) Rock:

Bearing strength : $f > 700 t/m^2$

Velocities of P and S waves : $V_p = 4.3$ km/sec.

$V_s = 2.3$ km/sec.

Specific gravity : $\rho_r = 2.5 t/m^3$

Poisson's ratio : $\nu_r = \dfrac{\rho_r (V_p/V_s)^2 - 2}{2[(V_p/V_s)^2 - 1]} = 0.3$

Young's modulus : $E_r = \dfrac{\rho_r}{g} \times V_p \times \dfrac{(1+\nu_r)(1-2\nu_r)}{(1-\nu_r)} = 3.5 \times 10^6 t/m^2$

Shear modulus : $G_r = V_s^2 \times \dfrac{\rho_r}{g} = 1.349 \times 10^6 t/m^2$ where $g = 980$ gal

c) Shape Factors for Shear Rigidity:

circle $\kappa = 4/3$ rectangle $\kappa = 1.5$

cylindrical shell $\kappa = 2.0$ I type $\kappa = 1.0 \sim 1.5$

d) Damping Factors:

Welded steel structure $h = 1\%$

Bolted steel structure $h = 2\%$

Concrete structure $h = 5\%$

e) Earthquake Waves:

		Duration of earthquake	
i) El Centro NS40	(E)	0 ~ 5 sec.	250 gal normalized
ii) Taft 52EW	(T)	0 ~ 10 sec.	
iii) Golden Gate S80E	(G)	0 ~ 5 sec.	

f) Rocking and Swaying Springs:

$$K_h = \frac{2 \cdot \pi}{2 - \nu_r} \times G \cdot a = 11.04 \times 10^7 t/m,$$

$$K_r = \frac{G \cdot a^3 \cdot \pi}{2(1 - \nu_r)} = 3.289 \times 10^{10} tm/rad.$$; where a is the radius of circular foundation.

These formulas are derived from Dr. Tajimi's theory developed for the flexible foundation on three-dimensional elastic medium (2).

The effective and additive mass of the hard rock underneath the foundation is not considered.

Table I - Input data of lumped mass and spring element

Interior Concrete Structure Mass 1-5

Property \ Lumped Mass Number		1	2	3	4	5
Mass	$m - \frac{T \cdot S^2}{M}$	2161.2	1897.0	1387.08	642.90	[illegible]
	$mr - T \cdot M \cdot S^2$	530169.94	465357.45	340239.1	157677.6	154076.1
	Xco-ord. - M	(-)51.1	(-)51.1	(-)51.1	(-)51.1	(-)51.1
	Yco-ord. - M	16.0	16.0	16.0	16.0	16.0
	Zco-ord. - M	*(2.87)	(5.73)	(7.4)	(7.0)	(8.3)
Vertical Spring	$Ax - M^2$	1387.88	1387.88	421.81	243.95	148.66
	$Ay - M^2$	1387.88	1387.88	421.81	243.95	148.66
	$Jx - M^4$	188957.69	188957.69	122592.21	9228.98	8365.4
	$Jy - M^4$	188957.69	188957.69	125820.82	21331.96	16303.7
	$Jp - M^4$	377915.4	377915.4	248413.0	30560.9	24669.1
	Xor - M	(-)51.1	(-)51.1	(-)51.1	(-)51.1	(-)51.1
	Yor - M	16.0	16.0	16.0	16.0	16.0
Horizontal Spring	$Kx - T/M\ 10^6$	(0-1) 7.25 (21-1) 11.39	(0-2) 6.44 (22-2) 3.56	(16-3) 15.97 (23-3) 4.28		
	$Ky - T/M\ 10^6$	3.07 26.9	2.73 8.40	13.21 10.08		
	$K\theta - T \cdot m/Rad.\ 10^6$	319.4 3587.4	283.93 1121.07	1150.75 1345.28		
	$\overline{X}or$ - M	(-)28.85 (-)51.1	(-)28.85 (-)51.1	(-)31.05 (-)51.10		
	$\overline{Y}or$ - M	16.00 (-)6.15	16.00 (-)6.15	26.00 (-)6.15		
	$\overline{X}'or$ - M	(-)28.75 (-)51.1	(-)28.75 (-)51.1	(-)30.05 (-)51.1		
	$\overline{Y}'or$ - M	16.00 (-)6.25	16.00 (-)6.25	26.0 (-)6.25		
Rocking Spring		Mass (0-1)				
	$Krx - T \cdot M/Rad.10^6$	32890				
	$Kry - T \cdot M/Rad.10^6$	32890				
Swaying Spring	$KHx - T/M\ 10^6$	110.4				
	$KHy - T/M\ 10^6$	110.4				
	$KH\theta - T \cdot M/Rad.10^6$	40623.0				
	Xor - M	(-)51.1				
	Yor - M	16.0				

Annulus Shield Wall Mass 6 ~ 10

Property \ Lumped Mass Number		6	7	8	9	10
Mass	$m - \frac{T \cdot S^2}{M}$	408.69	—	408.69	434.91	204.34
	$mr - T \cdot M \cdot S^2$	192437.9	—	192437.9	203840.1	96218.9
	Xco-ord. - M	(-)51.1	—	—	—	(-)51.1
	Yco-ord. - M	16.0	—	—	—	16.0
	Zco-ord. - M	*(13.6)	(13.6)	(13.6)	(13.6)	(13.6)
Vertical Spring	$Ax - M^2$	61.32	—	—	—	61.32
	$Ay - M^2$	61.32	—	—	—	61.32
	$Jx - M^4$	28889.4	—	—	—	28889.4
	$Jy - M^4$	28889.4	—	—	—	28889.4
	$Jp - M^4$	57778.8	—	—	—	57778.8
	Xor - M	(-)51.1	—	—	—	(-)51.1
	Yor - M	16.0	—	—	—	16.0

Steel Containment Vessel Mass 11~15

Property \ Lumped Mass Number		11	12	13	14	15
Mass	$m - \frac{T \cdot S^2}{M}$	53.2	53.2	87.3	18.3	15.4
	$mr - T \cdot M \cdot S^2$	19614.8	19614.8	24967.4	5971.84	1938.98
	Xco-ord. - M	(-)51.1	—	—	—	(-)51.1
	Yco-ord. - M	16.0	—	—	—	16.0
	Zco-ord. - M	*(14.5)	(14.5)	(14.5)	(12.25)	(12.25)
Vertical Spring	$Ax - M^2$	2.29	—	2.29	1.72	0.84
	$Ay - M^2$	2.29	—	2.29	1.72	0.84
	$Jx - M^4$	844.5	—	844.5	633.4	165.8
	$Jy - M^4$	844.5	—	844.5	633.4	165.8
	$Jp - M^4$	1689.1	—	1689.1	1266.8	331.6
	Xor - M	(-)51.1	—	—	—	(-)51.1
	Yor - M	16.0	—	—	—	16.0

Note : 1. *( ) mark shows the distance from the lower mass to the upper.

Table II - Natural period

CASE \ PERIOD (SEC)	STRUCTURE		1-ST	2-ND	3-RD	4-TH
CASE-1	INTERIOR CONCRETE STRUCTURE	X	0.0563 SEC	0.0226 SEC	— SEC	— SEC
		Y	0.0657	0.0229	—	—
	STEEL CONTAINMENT VESSEL	X Y	0.1616	0.0523	0.0344	0.0234
	ANNULUS SHIELD WALL	X Y	0.2756	0.0850	0.0475	0.0371
CASE-2	INTERIOR CONCRETE STRUCTURE	X	0.0739	0.0218	—	—
		Y	0.0779	0.0234	—	—
	STEEL CONTAINMENT VESSEL	X	0.1648	0.0524	0.0338	0.0234
		Y	0.1649	0.0526	0.0340	0.0221
	ANNULUS SHIELD WALL	X	0.2944	0.0899	0.0480	0.0379
		Y	0.2944	0.0908	0.0482	0.0362
CASE-3	INTERIOR CONCRETE STRUCTURE	X	0.0790	0.0276	—	—
		Y	0.0809	0.0283	—	—
	STEEL CONTAINMENT VESSEL	X	0.1670	0.0525	0.0344	0.0234
		Y	0.1671	0.0530	0.0344	0.0234
	ANNULUS SHIELD WALL	X	0.3090	0.0979	0.0485	0.0370
		Y	0.3090	0.0995	0.0471	0.0370
CASE-4	INTERIOR CONCRETE STRUCTURE	X	0.0726	0.0236	—	—
		Y	0.0787	0.0260	—	—
	STEEL CONTAINMENT VESSEL	X	0.1652	0.0524	0.0342	0.0236
		Y	0.1655	0.0525	0.0343	0.0233
	ANNULUS SHIELD WALL	X	0.2994	0.0905	0.0481	0.0369
		Y	0.3006	0.0932	0.0484	0.0370

Note: The modes of C - 2 ~ C - 4 in this table are selected as equivalent to those of C - 1.

Nomenclature in Table 1

m = Lumped mass ;

mr = Mass inertia about C.G. ;

Xco-ord. Yco-ord. - Co-ordinate of C.G. of lumped mass ;

Zco-ord. = Distance between the lower mass and upper one ;

Ax, Ay - Cross sectional area ;

Jx, Jy - Moment of inertia in x, y direction ;

Jp - Polar moment inertia ;

Xcr, Ycr Co-ordinate of vertical spring in x, y direction ;

Kx, Ky = Stiffness in x, y direction ;

Kθ = Torsional stiffness ;

$\overline{X}cr$, $\overline{X}'cr$ = Co-ordinate of 2 end points of horizontal spring in x direction ;

$\overline{Y}cr$, $\overline{Y}'cr$ = Co-ordinate of 2 end points of horizontal spring in y direction ;

Krx, Kry = Rocking spring of a rock in x, y direction ;

KHx, KHy = Swaying spring of rock in x, y direction ;

KHθ = Torsional spring of a rock ;

5. Results and Discussions

The mode shapes multiplied by participation factors for C - 2~C - 4, and responses and stresses for C - 1~C - 4 due to three earthquake waves are shown in Figs.6a~6b, and Figs. 7a~7c respectively, but, for want of space, the model shapes of C - 2~C - 4, and responses and stresses for X-direction earthquake waves are described and among many mode shapes some of them sufficiently enough to show the modes corresponding to the 1st. of ICS, the 1st.~2nd. of SCV, and the 1st.~3rd. of ASW proper respectively, are selected.

The stresses both in X-direction by X-waves and in Y-direction by Y-waves at the time of the maximum foundation rotation are shown in Fig.8.

a) Eigen values:

Among the natural periods of three structural components(Table II), those of ASW is the largest followed by SCV and ICS. The natural periods according to the differences among the models are found in the following order of cases:

C - 3 > C - 4 > C - 2 > C - 1.

The natural periods of C - 1 are much different from those of other three cases. The natural periods of C - 4 are almost same as those of C - 2, as RCF in C - 4 is restrained around the boundary of its foundation by the horizontal springs. Nevertheless, natural mode shapes multiplied by participation factors (Figs. 6a, and 6b) are close one another.

b) Response values:

The maximum response accelerations and maximum relative displacements of each structural component are shown in Figs. 7a~7c.

The maximum response accelerations and maximum relative displacements in each structural component are found in the following order of components: SCV > ASW > ICS and ASW > SCV > ICS respectively. Those due to differences among models through the excitations of all three earthquake waves are both found in the following order of the cases: C - 3 > C - 4 > C - 2 > C - 1.

The greatest values of the maximum response accelerations by three earthquake waves for C - 1 are about 71% in ICS, 67% in SCV, and 64% in ASW compared with those for C - 3, and the greatest values of the maximum relative displacements by three earthquake waves for C - 1 are about 16% in ICS, 55% in SCV, and 62% in ASW compared with those for C - 3. These three earthquake waves concerned, the magnitudes of the maximum response accelerations and relative displacements in four cases are, on the whole, observed in the following order: T > G > E in SCV, E > T > G in ASW, but not pronounced significantly in ICS (Tables III, and IV).

Table III - Comparison of max. response acceleration at top mass

Str.	Wave dir.	C - 3 >	C - 4 >	C - 2 >	C - 1	C-2, C-3, C-4	C-1
ICS	X	(1.0) E:600gal	(0.80) E:480gal	(0.75) E:450gal	(0.73) T:440gal	(1.0)(0.92)(0.68) E > G > T	(1.0)(0.78)(0.71) T > G > E
	Y	(1.0) E:630gal	(0.86) E:540gal	(0.77) E:480gal	(0.68) T:430gal	(1.0)(0.94)(0.75) E > G > T	(1.0)(0.86)(0.84) T > E > G
SCV	X	(1.0) T:2350gal	(0.89) T:2090gal	(0.85) T:1990gal	(0.70) T:1650gal	(1.0)(0.87)(0.64) T > G > E	(1.0)(0.94)(0.91) T > G > E
	Y	(1.0) T:2600gal	(0.84) T:2190gal	(0.80) T:2070gal	(0.64) T:1650gal	(1.0)(0.84)(0.64) T > G > E	(1.0)(0.94)(0.91) T > G > E
ASW	X	(1.0) E:1510gal	(0.85) E:1280gal	(0.76) E:1150gal	(0.64) E:960gal	(1.0)(0.93)(0.74) E > T > G	(1.0)(0.92)(0.83) E > T > G
	Y	(1.0) E:1480gal	(0.89) E:1310gal	(0.78) E:1170gal	(0.65) E:960gal	(1.0)(0.85)(0.76) E > T > G	(1.0)(0.92)(0.83) E > T > G

Figures in ( ) shown for C - 3 only

Table IV - Comparison of max. response displacement at top mass

Str.	Wave dir.	C - 3 >	C - 4 >	C - 2 >	C - 1		C-2, C-3, C-4	C-1
ICS	X	(1.0) T:0.294cm	(0.61) T:0.178cm	(0.49) T:0.144cm	(0.14) T:0.041cm	...	(1.0)(0.92)(0.55) T > E > G	(1.0)(0.84)(0.72) T > G > E
	Y	(1.0) T:0.303cm	(0.66) T:0.201cm	(0.51) E:0.155cm	(0.17) T:0.051cm	...	(1.0)(0.95)(0.61) T > E > G	(1.0)(0.89)(0.88) T > E > G
SCV	X	(1.0) T:2.00cm	(0.81) T:1.61cm	(0.74) T:1.48cm	(0.55) T:1.10cm	...	(1.0)(0.70)(0.59) T > G > E	(1.0)(0.94)(0.89) T > E > G
	Y	(1.0) T:2.00cm	(0.82) T:1.64cm	(0.75) T:1.49cm	(0.55) T:1.10cm	...	(1.0)(0.69)(0.59) T > G > E	
ASW	X	(1.0) T:2.70cm	(0.86) T:2.32cm	(0.77) T:2.09cm	(0.62) E:1.66cm	...	(1.0)(0.98)(0.62) T > E > G	(1.0)(0.96)(0.79) E > T > G
	Y	(1.0) T:2.70cm	(0.88) T:2.38cm	(0.75) T:2.01cm	(0.62) E:1.66cm	...	(1.0)(0.98)(0.62) T > E > G	

Figures in ( ) shown for C - 3 only

The differences of those values are rather considerable. The relative displacements of ICS for C - 1 deviate greately compared with those of other cases according to the fixing condition of the base.

Consequently, C - 3 or C - 4 shall be used to make the floor response spectrum to be applied to the aseismic designs of equipments and piping systems, etc., and much studies must be done for the proper selection of earthquake waves suitable for the plant site.

c) Stresses:

The resultant maximum shears and bending moments by three earthquake waves are shwon in Figs. 7a~7c. The maximum shear stresses concerned, C - 3 > C - 4 > C - 2 > C - 1 is found in the order of the components. The maximum bending moments concerned, C - 3 > C - 4 > C - 2 > C - 1 is found in the order for ICS and ASW, and C - 4 > C - 3 > C - 2 > C - 1 for SCV. On the average, the maximum resultant shears on the top of the foundation for C - 1 are about 59% in ICS, 73% in SCV, and 74% in ASW to those for the leading case, either C - 3 or C - 4.

The earthquake waves concerned, the order in the magnitudes of both the maximum resultant shear and bending moment are T > G > E in SCV, T > E > G in ASW except for C - 1, and not pronunced significantly in ASW for C - 1 and in ICS for all cases (Tables V, and VI). By the comparison of the stresses corresponding to E, T, and G, the stresses are much different one other. Judging from the above comparisons, structural modeling, such as C - 3 or C - 4 shall be required to attain reasonable structural design in case of the time history response analyses.

Table V - Comparison of max. resultant shear stress on top of foundation.

Str.	Wave dir.	C - 3 >	C - 4 >	C - 2 >	C - 1		C-2 , C-3 , C-4	C-1
ICS	X	(1.0) G:7680ton	(0.80) E:6150ton	(0.75) E:5720ton	(0.61) T:4650ton			
	Y	(1.0) G:7800ton	(0.82) E:6400ton	(0.74) T:5760ton	(0.57) T:4420ton			
SCV	X	(1.0) T:2750ton	(0.98) T:2700ton	(0.92) T:2540ton	(0.74) T:2030ton	...	(1.0)(0.81)(0.66) T > G > E	(1.0)(0.79)(0.77) T > G > E
	Y	(1.0) T:2820ton	(0.98) T:2760ton	(0.91) T:2560ton	(0.72) T:2030ton	...	(1.0)(0.81)(0.67) T > G > E	
ASW	X	(1.0) T:12700ton	(0.96) T:12200ton	(0.87) T:11000ton	(0.70) E:8860ton	...	(1.0)(0.92)(0.63) T > E > G	(1.0)(0.97)(0.89) T > E > G
	Y	(1.0) T:12700ton	(0.96) T:12200ton	(0.86) T:10940ton	(0.70) E:8860ton	...	(1.0)(0.88)(0.59) T > E > G	

Figures in ( ) shown for C - 3 only

Table VI - Comparison of max. resultant bending moment on top of foundation

Str.	Wave dir.	C - 3 >	C - 4 >	C - 2 >	C - 1		C-2, C-3, C-4	C-1
ICS	X	(1.0) G:91200tm	(0.81) E:74300tm	(0.78) E:70800tm	(0.60) T:55100tm			
	Y	(1.0) G:93100tm	(0.84) E:78000tm	(0.76) E:70800tm	(0.58) T:53600tm			
ASW	X	(1.0) T:567000tm	(0.89) T:506700tm	(0.83) T:470000tm	(0.74) E:416200tm	...	(1.0)(0.97)(0.59) T > E > G	(1.0)(0.95)(0.79) E > T > G
	Y	(1.0) T:569000tm	(0.91) T:515000tm	(0.83) T:470500tm	(0.73) E:416000tm	...	(1.0)(0.97)(0.59) T > E > G	

Figures in ( ) shown for C - 3 only

Str.	Wave dir.	C - 4 >	C - 3 >	C - 2 >	C - 1		C-2 C-3 C-4	C-1
SCV	X	(1.0) T:112000tm	(0.91) T:111700tm	(0.90) T:106400tm	(0.72) T:86500tm	...	(1.0)(0.88)(0.68) T > G > E	(1.0)(0.94)(0.91) T > G > E
	Y	(1.0) T:113700tm	(0.99) T:112600tm	(0.94) T:107000tm	(0.74) T:86500tm	...	(1.0)(0.88)(0.68) T > G > E	

Figures in ( ) shown for C - 4 only

d) Base shears and bending moments beneath the RCF foundation:

As the direct comparison on the base shears and bending moments for C - 1 with other cases will not be so effective theoretically, C - 1 is not discussed in this section. The cases in which the maximum base shears caused by three earthquake waves, are found C - 3 > C - 2 > C - 4 in the order, and the values corresponding to the cases are in the ratio about 1.0 : 0.7 : 0.4 (Table VII). The order of the earthquake waves causing the maximum base shears is T > E > G in X-direction except for C - 4, and the maximum value for T is almost same as for E and much greater than for G. The cases in which maximum overturning moments and the maximum rotational angles of RCF foundation (Table XI) are caused, are C - 3 > C - 2 > C - 4 in the order, and the values corresponding to the cases are in the ratio about 1.0 : 0.84 : 0.70 (Table VIII). In C - 4, it is understood that the large shear forces are transferred to the Attached Buildings through the horizontal springs, as shown in Fig.8. Table XI shows maximum stresses in these horizontal springs due to T of a typical response. It should be noted that the stability of RCF is much increased in such a manner (Comp. Figs. 7b, and 8).

Considering the magnitudes of stresses in these horizontal springs between RCF and AB, reasonable and suitable estimations of rigidities for them should be required in practical designs.

Even when studies as above for C - 4 is not taken, proper reinforcings for horizontal springs are desirable. The overturning moments of RCF concerned, we can say, evaluations by C - 3 will be very convienient and properly conservative procedure.

Table VII - Comparison of max. base shear

Wave dir.	C - 3 >	C - 2 >	C - 4		C - 3	C - 2	C - 4
X	(1.0) T:24590ton	(0.68) T:16800ton	(0.37) E:9020ton	...	(1.0)(0.96)(0.72) T > E > G	(1.0)(0.99)(0.62) T > E > G	(1.0)(0.94)(0.93) E > G > T
Y	(1.0) T:24060ton	(0.69) T:16620ton	(0.44) T:10688ton	...	(1.0)(0.99)(0.94) T > E > G	(1.0)(0.99)(0.62) T > E > G	(1.0)(0.99)(0.84) T > E > G

Table VIII - Comparison of max. overturning moment

Wave dir.	C - 3 >	C - 2 >	C - 4	C - 3	C - 2	C - 4
X	(1.0) T:942200tm	(0.84) T:791000tm	(0.68) T:643800tm	(1.0)(0.87)(0.54) T > E > G	(1.0)(0.86)(0.64) T > E > G	(1.0)(0.89)(0.65) T > E > G
Y	(1.0) T:939600tm	(0.83) T:780800tm	(0.72) T:673300tm	(1.0)(0.86)(0.53) T > E > G	(1.0)(0.86)(0.66) T > E > G	(1.0)(0.88)(0.64) T > E > G

Table IX - Max. stress of horizontal spring for C - 4 by T

Horizontal spring	3 — 16			3 — 23			2 — 0		
Wave direction	Axial str.	Shear str.	Bending moment	Axial str.	Shear str.	Bending moment	Axial str.	Shear str.	Bending moment
X	7232t	675t	3659tm	200t	1275t	2664tm	1649t	44t	368tm
Y	1091t	6123t	8173tm	675t	415t	7223tm	59t	531t	510tm

Horizontal spring	2 — 22			1 — 21		
Wave direction	Axial str.	Shear str.	Bending moment	Axial str.	Shear str.	Bending moment
X	43t	257t	1381tm	159t	652t	2168tm
Y	322t	57t	876tm	1541t	202t	7939tm

Table X - Occurrence times for max. response and stress for C - 1~4 (Sec.)

Structural components	Earthquake wave	Maximum acceleration	Maximum displacement	Maximum shear	Maximum moment
ICS	E	2.34	2.01 – 2.59	2.34 – 3.60	2.33 – 2.34
	T	4.54 – 8.02	6.59 – 6.76	4.54 – 8.1	4.53 – 6.52
	G	1.47 – 2.59	1.48 – 2.60	1.47 – 2.76	1.44 – 1.70
SCV	E	3.43 – 3.66	1.99 – 3.98	2.63 – 3.98	2.63 – 3.97
	T	7.84 – 8.47	8.47 – 9.50	8.47 – 9.84	8.46 – 9.34
	G	1.66 – 2.23	1.63 – 2.65	1.79 – 2.65	1.68 – 2.64
ASW	E	2.54	2.45 – 3.05	2.55 – 3.79	2.53 – 2.55
	T	4.95 – 9.34	4.95 – 9.33	6.57 – 9.48	4.99 – 9.33
	G	1.67 – 1.54	1.55 – 1.66	1.67 – 2.86	1.55 – 1.70

Earthquake wave	Maximum base shear	Max. overt. moment	Horizontal spring stress
E	2.01 – 2.59	2.01 – 2.02	2.02 – 3.98
T	6.59 – 6.60	6.59 – 9.50	4.90 – 9.99
G	1.48 – 1.55	1.55 – 1.56	1.47 – 2.84

e) The responses torsional and normal to the earthquake waves:

The maximum responses both torsional and normal to the earthquake waves can be seen from the results of responses for C - 4 (Fig. 7c).

For example, the torsional acceleration of ASW is 0.0345rad./sec.^{2} and the tangential acceleration on the internal face derived accordingly is 74gal. The ratios between the maximum responses normal and parallel to the earthquake waves are less than 1 : 5 in ICS, 1 : 15 in SCV, and 1 : 25 in ASW. These phenomena are not so critical but should be taken into account in practical structural designs for buildings complicated.

f) Time of maximum responses and stresses:

The ranges of time, during which the maximum responses are attained due to three earthquake waves for each structural component, are shown in Table X. The durations of the earthquakes (Chap. 4, c)) planned for computation at the beginning of this study are verified reasonable by those values.

Table XI - Max. rotational angle of RCF foundation ($\times 10^{-4}$ rad.)

Earthquake wave	C - 3		C - 4	
	X-dir.	Y-dir.	X-dir.	Y-dir.
E	0.269	0.265	0.174	0.179
T	0.309	0.309	0.196	0.205
G	0.168	0.164	0.127	0.131

6. Conclusions

It is concluded from the present studies that:

1) In many respectes, the responses for C - 4 range between those for C - 2 and for C - 3, and the stability of RCF is much increased for C - 4.
The above fact is naturally expected from the restraints around the boundary of RCF foundation.

2) The modeling of C - 3 is the most conservative of the four modelings, and can be said to be simple and proper for structural design of a building complicated such as a nuclear power station.

3) However, the RCF - AB interaction effects by earthquake excitation should be taken into consideration in practial design of the RCF - AB junction.

For the fundamental planning of the layout of the nuclear power station, structural engineers shall be joined in the planning from the beginning to make the layout simple for analytical modelings in order to develope more adequate engineering for structural designs.

Acknowledgement

The writers wish to express paticular thanks to Dr.Hiroshi Tajimi, Professor of Nihon University for helpful suggestions.

R e f e r e n c e s

[1] H. Tajimi,
Introduction to Structural Dynamics (Japanese),
Corona Book Co., September, 1966.

[2] K. Kanai, H. Tajimi and others,
Series of Structural Design; Vol.1, Engineering Seismology (Japanese),
Shokoku-sha Book Co., November, 1968.

[3] K. Muto,
Series of Aseismic Design; Vol.4, Dynamic Analysis of Structures (Japanese),
Maruzen Book Co., August, 1963.

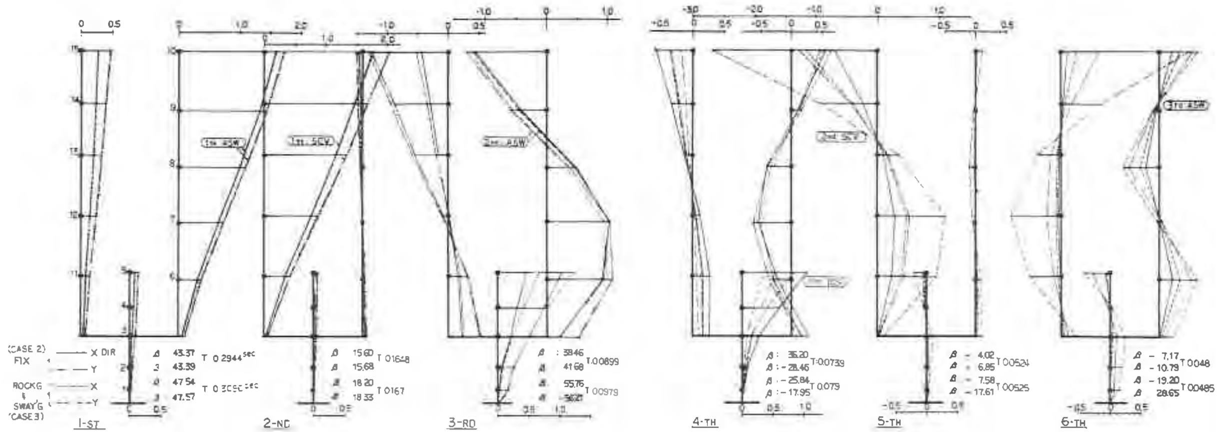

Fig. 6a The mode shapes multiplied by participation factors in X-direction in C - 2, and C - 3

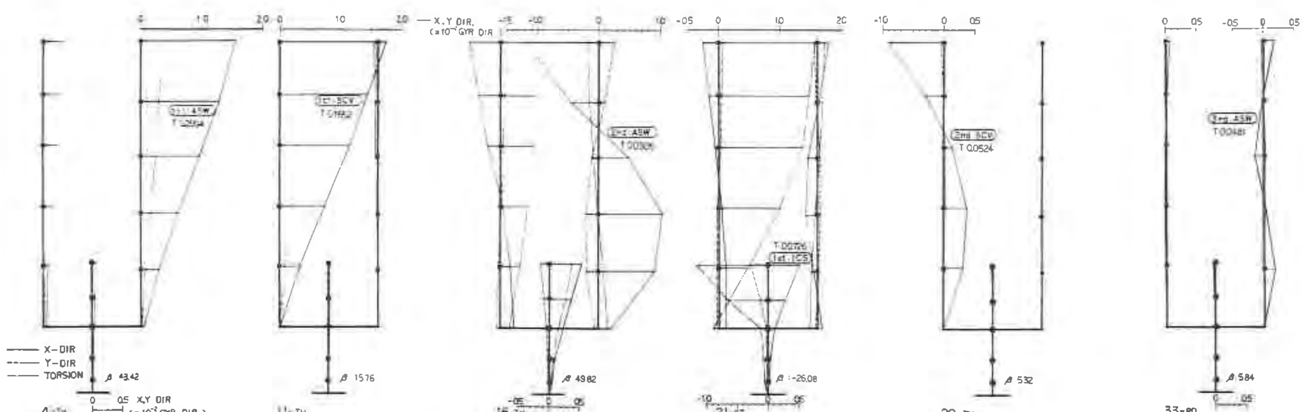

Fig. 6b The model shapes multiplied by participation factors in X-direction in C - 4

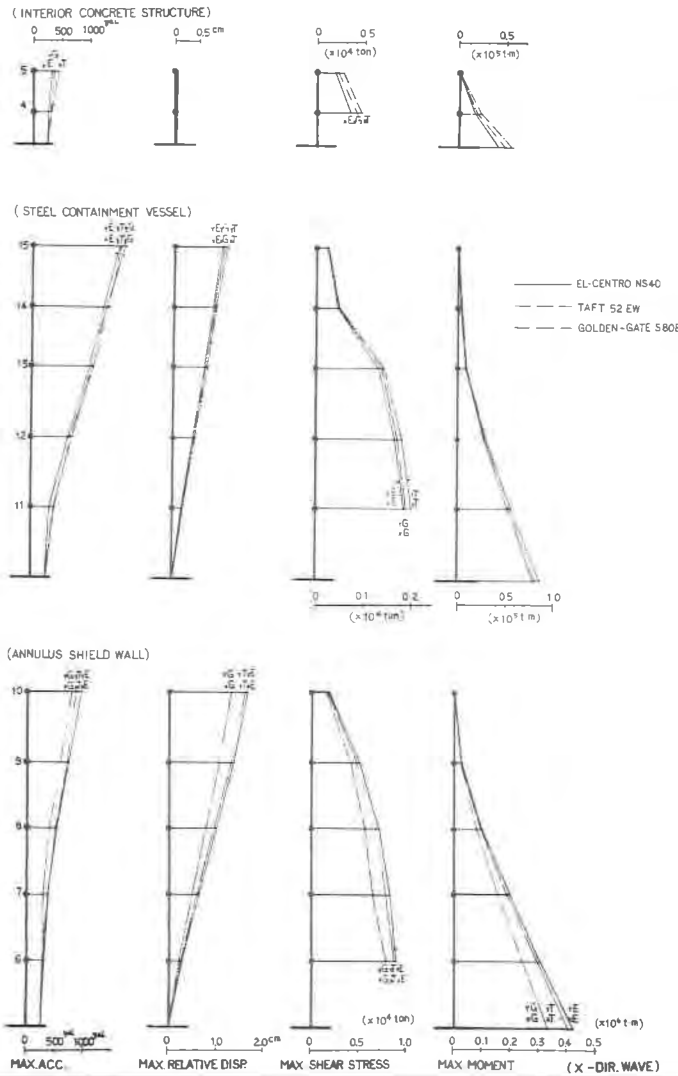
(INTERIOR CONCRETE STRUCTURE)
(STEEL CONTAINMENT VESSEL)
(ANNULUS SHIELD WALL)
EL-CENTRO NS40
TAFT 52 EW
GOLDEN-GATE S80E
MAX.ACC.
MAX.RELATIVE DISP.
MAX.SHEAR STRESS
MAX.MOMENT
(X-DIR.WAVE)

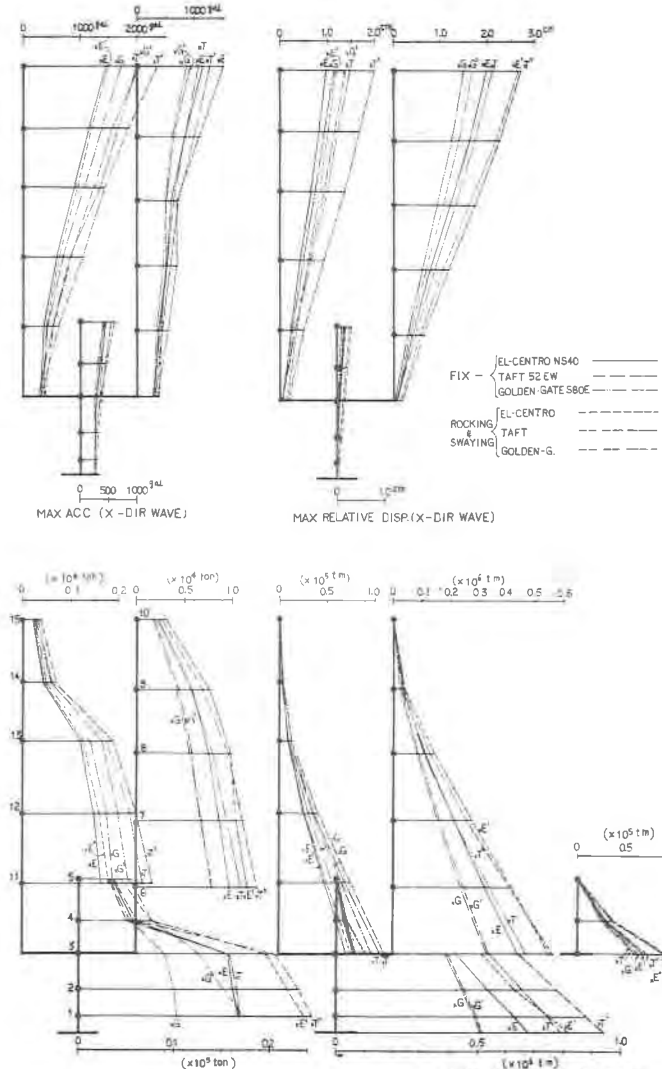
FIX – EL-CENTRO NS40
TAFT 52 EW
GOLDEN-GATE S80E
ROCKING & SWAYING EL-CENTRO
TAFT
GOLDEN-G.
MAX ACC (X-DIR WAVE)
MAX RELATIVE DISP.(X-DIR WAVE)
MAX SHEAR STRESS (X-DIR WAVE)
MAX MOMENT (X-DIR WAVE)

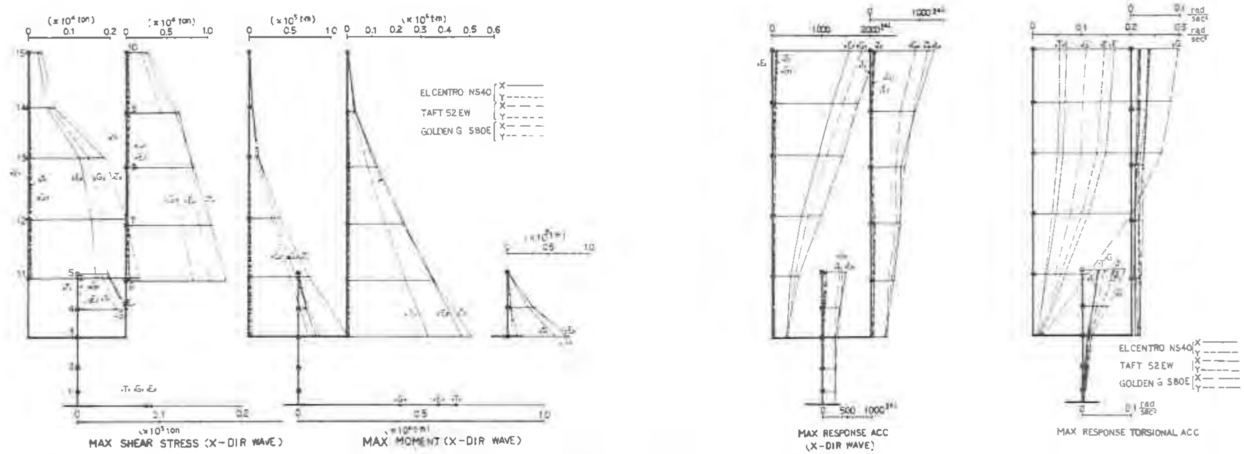

Fig. 7c Max. responses and stresses for C - 4

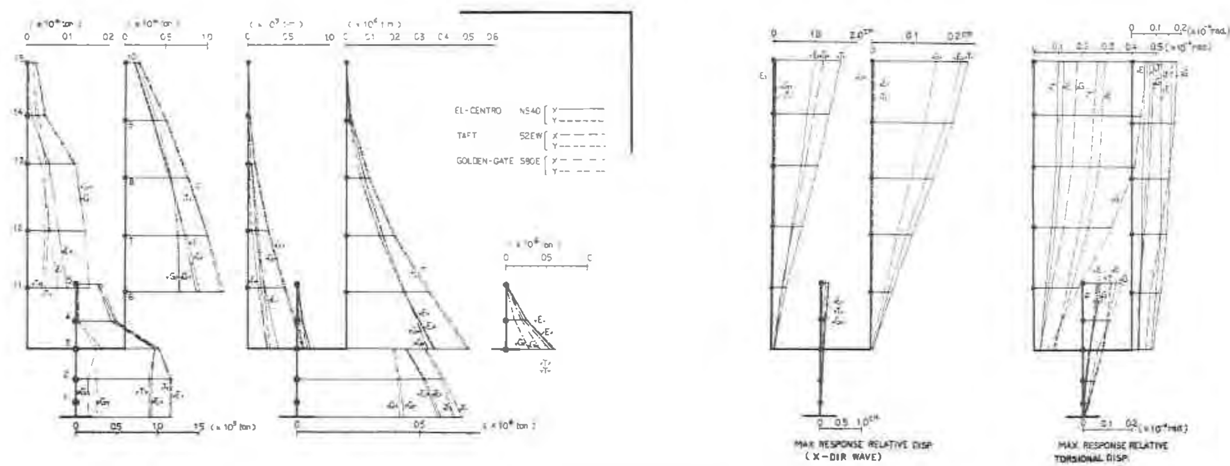

Fig. 8 The stresses at the time of the maximum rotation angles of RCF foundation